Design and manufacturing of a Linear Induction Motor for the 2019 EPFLoop prototype in the framework of the SpaceX Hyperloop competition

Martin Seydoux, Nicolò Riva, Simone Rametti, Lorenzo Benedetti,

Theophane Dimier, Nicolas Bollier, André Hodder

EPFL and EPFLoop

Abstract: The EPFLoop team from Ecole Polytechnique Fédérale de Lausanne has developed a capsule thanks to which won the 3rd place at the SpaceX Hyperloop Pod Competition in 2018 edition and the 3rd place in the 2019 edition. For the 2019 competition our team decided to design, develop and assemble a propulsion system composed of a Double-Sided Linear Induction Motor (DSLIM). This kind of propulsion offers numerous advantages, removing the need for a direct contact propulsion mechanism (which provides a significant weight reduction) along with any dependence on maintaining contact between such a mechanism and the rail. Since its performance can be studied and improved analyzing material properties or geometrical factors, in this contribution we describe the approaches that have been followed using COMSOL to provide an accurate estimation of the main figure of merit, namely the exerted thrust. An optimization process has been carried out based on simulation results. The goal was to find the best motor geometry and configuration in terms of maximum capsule speed, which in turn consists in finding the maximum thrust force for the given supply frequency and current at a certain speed. The simulations are then compared with experimental measurements carried out on the motor at EPFL and during the final run. The outcome is a complete study, design and manufacturing of a LIM considering magnetic saturation, spatial field harmonics, leakage flux, pole pitch, total air gap, input frequency, material resistivities and eventually "End Effects". The simulation results have been carried out by using the AC/DC module (Magnetic Field and Magnetic Electric Field) for 2D/3D models.

Keywords: Hyperloop, SpaceX, EPFL, EPFLoop, Propulsion , LIM

1. Introduction

The concept of Hyperloop Alpha concept has been proposed in an open source paper published by Elon Musk and SpaceX [1], as a passenger or goods high-speed rail system. The Hyperloop can satisfy a growing need for transportation on short-middle travel. For instance, on the Bern-Zürich (123 km) route the traveling time can be reduced to 9 minutes. The Hyperloop Pod Competition, created by SpaceX in 2015, aims to encourage innovation and to improve the development of a working prototype. This work describes how the EPFLoop team used COMSOL Multiphysics to analyze and study the design choices of the linear induction motor of their prototype, which allowed to build and test a prototype, winning the 3rd place in the SpaceX Hyperloop competition 2019.

2. Governing equation and design approach

a. Concept of a double side LIM

For rotatory induction machine, the synchronous speed can be assimilate to a speed where no-torque is created (T=0). This is explained by the fact that no currents are induced in the rotor as long as the rotating magnetic field and the rotor share the same rotational speed. A *slip factor* is defined to take into account the difference of speed between the rotor and the speed of the rotating magnetic field. Thus slip is equal to zero (s=0) for such synchronous speed and no torque is created. For a linear induction motor, this slip is defined as the difference between the speed of the travelling magnetic field created by the inductors and the speed of the rail (place where the currents are induced). The relation can express the linear speed of the moving magnetic field:

$$V_{magnetic\,field} = 2 \cdot \tau_p \cdot f$$

where τ_p is the pole pitch, which is the distance between the central line of one pole to the central line of the next pole. In a LIM, due to "end effects", a braking force is present for such synchronous speed. The linear induction technology appeared nearly a century ago, but its use is not widely spread due to the low efficiencies. In fact, to avoid friction between the primary (the copper coils and the iron core) and the secondary (the rail in which the field is induced), a sufficiently large air gap is required. However, having a large air-gap compared to the pole pitch of the motor leads to an increase of leakage flux and, thus, a drastic decrease of the thrust. In addition, in a LIM, the finite length of the primary or secondary implies that the flux immediately ahead and behind the pod will be lost, reducing the amount of active power. This results in a reduction of the flux and, consequently, of the thrust. However, this type of propulsion has the undeniable advantage of not depending on the adherence, therefore external conditions have a very limited impact on the performances of the propulsion system. This allows ensuring a given thrust even in harsh environment, where the rail conditions are expected to be poor.

The design of the linear induction motor begins considering the constraints imposed by the SpaceX Hyperloop track and the competition rules. Even if the design of the prototype is not bound in the framework of the competition, the geometry of the rail is fixed and it is an I-shaped beam made out of aluminum AW 6061-T6. This forces the design of a LIM to two main possibilities, namely a top placed single inductor or a double-sided inductors motor (Figure 1). The latter design can help in limiting the amount of leakage flux reducing the component of the varying vertical force. This in fact would change the force applied during the run on the stability system, resulting in a major change of the air gap and thus affecting the performance of the prototype. The second design instead creates a symmetrical load that can easily be handled by the frame of the prototype. Knowing the complexity and sensitivity on the performances of the propulsion an extended study has been realized in order to provide a solution with the most performant motor, optimizing the thrust characteristics.

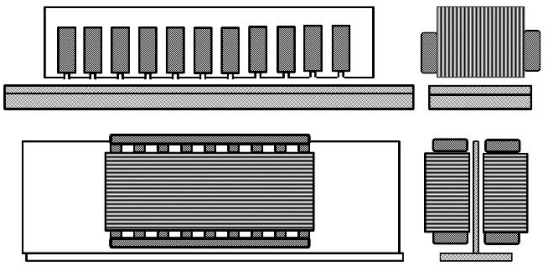

Figure 1: Possible configuration of a LIM.

b. **Rationale behind the design**

The use of COMSOL Multiphysics allowed to perform a study depending on numerous parameters, in order to understand whether and to what extent the parameters impact on the electromagnetic thrust and efficiency. The performance of the motor is strongly affected by the air-gap: the closer the inductors are to the rail, the bigger the thrust is. Nevertheless, due to misalignment of the manifold section of the rail, the tolerances of the beam and the natural oscillations of the prototype during the run, the distance in between an inductor and the rail must be fixed to 5 mm. In fact, a smaller distance would be critical since the prototype vibrations would result into an unwanted collision of the motor with the rail, and a larger distance would decrease dramatically its performances.

3. Design of the double-sided LIM through a 2D finite element model

In this section, we will first present the sizing of the pole pitch and the number of pole constituting the motor using COMSOL. Despite a 3D model was developed in collaboration with COMSOL, the design has been studied and developed in 2D, evaluating the magnetic flux configuration on the transversal plane (Figure 2). In fact, a complete study of the LIM in 3D for all the speed and frequency was not compatible with the tight timeline at our disposal. In the last stage, preliminary 3D studies have been carried out with such a model, in order to evaluate properly the end effects on all the motor, but for the sake of brevity in this

contribution, we will present only the 2D analysis. The approximation of the 2D model in fact is acceptable for the level of accuracy that we required at the initial stage of the design. The side effects have a smaller impact on performances compare to what other parameters have such as teeth geometry, number of teeth, pole pitch.

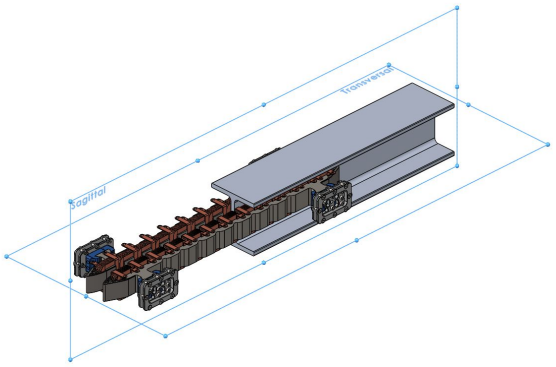

Figure 2: Motor and rail with reference plane.

a. **Geometry and material properties**

The geometry has been parametrically built in order to tune the parameters of the design such as the number of teeth, the pole pitch, the geometry of the slot and coils. The geometry built and simulated in COMSOL is composed by the AW6061-T6 aluminum domain, representing half of the rail (thickness: 5.2 mm), a set of copper coils, the iron core supporting the windings and the surrounding air. The aluminium and copper properties were implemented in the COMSOL library. The conductivity of the air has been set to 0 S. The core of the motor was realized of a stacked sheet of magnetic steel NO20-13HS of 0.2 mm thickness ensuring low core losses even with frequency above a few tenths of Hertz. Since the losses in the iron are small compared to the Joules losses induced in the rail, the electrical conductivity of the iron has initially been set to 0 S to guarantee no circulating induced currents in the main core of the motor. However, this affected the numerical stability of the model, therefore the value has been changed to 0.1 S.

The non-linear saturation of the iron has been simulated with the *B-H curve* and *Effective B-H curve* features of the Magnetic Field (*mf)* module. Waelzholz has provided the B-H curve of the iron core.

b. **Module used, boundary condition and solver**

The Magnetic Field *(mf)* module has a built-in interface allowing to represent the behavior of a coil. The selected coil typology is the *Homogenized multi-turn coil,* where the current in the slot is represented via a current density, an area and a filling factor. To represent properly the three phases of the electrical machine, three groups of coils have been defined as it follows:

$$Ie^{-\frac{2}{3}k\pi j}$$

where I is the current, k=1,2,3 and the exponential represents the phasor. The filling factor represent the capability of the windings to fill the slot. In general, this coefficient does not overcome 50 % for cylindrical wire made in large series. Nevertheless, by machining with CNC machine raw copper and ending up with rectangular cross section, this factor has been increased up to 73 %.

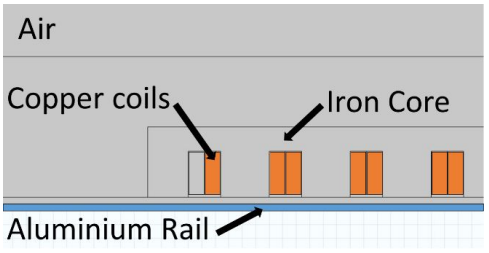

Figure 3: Detail of the 2D simulated geometry.

To simulate the movement of the motor with respect to the rail, two approaches are possible. Simulating a moving domain can result into a very complicated simulation, where Moving Meshes, Magnetic Field and ODEs are involved. In order to avoid such complexity COMSOL developed the *Velocity (Lorentz Term)* feature, used to describe the translational velocity. This remarkable feature takes into account the induction caused by

stationary magnetic sources in a moving domain, without introducing complexities such as moving mesh. Induction in our case is caused by the variation of the magnetic field (i.e. the current), the frequency and, hence, the speed. The induced current density in the selected domain are calculated as:

$$J = \sigma(E + v \wedge B)$$

Sweeping on the velocity and evaluating a frequency domain study it is possible to evaluate the variation of thrust at each pair [v,f]. The thrust is calculated firstly computing the linear Maxwell stress tensor:

$$\sigma_{ij} = \varepsilon_0(E_i E_j - \tfrac{1}{2}\delta_{ij}E^2) + \tfrac{1}{\mu_0}(B_i B_j - \tfrac{1}{2}\delta_{ij}B^2)$$

and, then, performing the volume integration over the domain of the motor, that is where electric and magnetic fields are generated:

$$F = \int n \cdot \sigma \, d\Omega$$

The calculation, realised over the motor (coil & iron core) or over the aluminium rail, is equivalent and provides the same resultant with opposite sign, since in the air domain no relevant electromagnetic phenomenon is expected to occur. Referring to Figure 2 (sagittal plane) the symmetry of the motor allowed simulating only half of the geometry, reducing the computation time of simulation. In order to take into account of such symmetry, a *perfect magnetic conductor* $(n \wedge H = 0)$ boundary condition has been applied. This boundary condition sets the tangential component of the magnetic field **H** to zero and enforces that the magnetic field can have no tangential component as it approaches the boundary, so the magnetic field can only point in the normal direction and cannot change sign as you cross the boundary. Physically this represents the magnetic flux going from one tooth to the facing tooth through the rail. On the external boundaries instead, a *magnetic insulation* $(n \wedge A = 0)$ boundary condition has been applied by default. This boundary condition sets the normal component of magnetic field **H** to zero, hence, enforcing that the magnetic field must be tangential to this boundary.

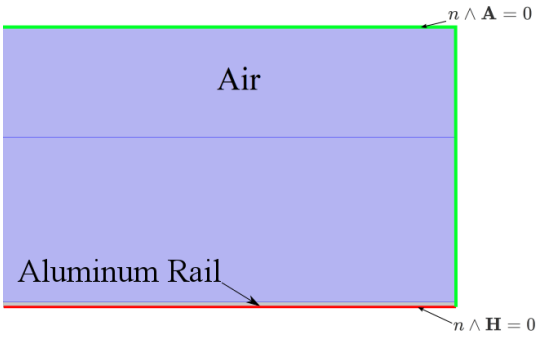

Figure 4: Boundary conditions.

As a consequence, this boundary condition has the physical interpretation of a boundary through which current can only flow in the normal direction.

A larger distance from the domain boundaries was considered behind the LIM $(\sim 3 \cdot L_{pod})$ than in front of it $(\sim 1 \cdot L_{pod})$. However, such lengths are not sufficient to capture the magnetic flux at every speed and frequency along the rail and typically larger domains must be considered. Larger domains however would affect the computational time since it would increase the number of elements and therefore the DOF. To avoid such complexity we used another advantageous feature of COMSOL. The geometry has been surrounded by an air domain where the *infinite domain* condition has been applied. The advantage of the infinite element domain is that it obviates the question of choosing between boundary conditions as well as the question of the domain size. The solution from a model with infinite element domains will be the same as when the domain radius is increased. A *Fully Coupled* approach with a *Direct Solver* has been used as settings for the frequency domain study.

c. **Mesh**

In simulating electromagnetic phenomena such as the skin effect into the rail, the mesh quality should be carefully considered. In fact, the equivalent impedance of the rail has a large impact on the performance of the induction machine. For this reason, knowing the

maximum frequency supplied, the size of rail's elements was set to half of the induced current penetration:

$$V_{element} = \frac{1}{2\sqrt{\sigma\mu f}}$$

σ is the electrical conductivity in S/m and μ the magnetic permeability in H/m. For instance, with the maximum frequency of 900 Hz, the conductivity of the aluminium of $\sigma = 25 \cdot 10^6$ and a permeability μ=1, we have $V_{element} = 3.33 \cdot 10^{-6}$. The mesh size is particularly fine in the area where the magnetic flux varies in a significant manner and depends on the frequency. In Figure 6 it is possible to see the different mesh sizes depending on the simulated domain, where the highlighted blue area is the air domain. Eventually, the length of the model was set to at least three times the length of the motor in order to take into account the tail effect, namely to capture the magnetic flux travelling along the rail.

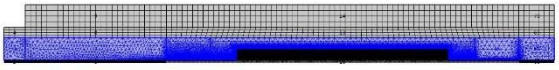

Figure 5: Mesh of the entire domain

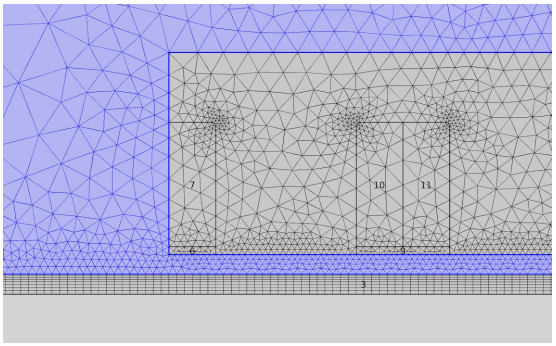

Figure 6: Mesh in the air-gap (blue highlighted), motor and rail (quad mesh domain).

4. Results and experimental validation

The study was performed by fixing the current and evaluating the thrust profile for a given speed and a given supply frequency. The Figure 7 shows the thrust for a fixed speed of 50 m/s in function of the frequency.

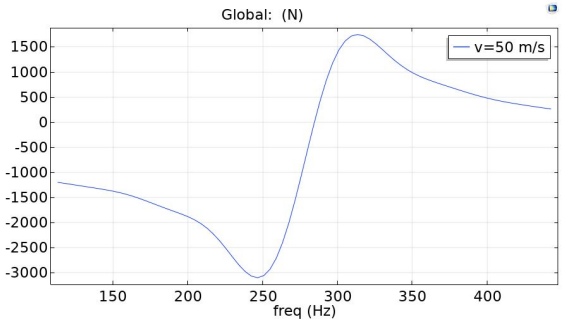

Figure 7: Thrust characteristic for a fixed speed with respect to supply frequency.

Knowing that the pole pitch of the model used for the plot is 0.09 m, and the speed is set to 50 m/s, the synchronous frequency in order to have a moving magnetic field going at the same speed as the rail is :

$$f = \frac{v}{2 \cdot \tau_p} = \frac{50}{2 \cdot 0.09} = 277.\overline{7}\ \text{Hz}$$

As shown in Figure 7 the amplitude of the force at this synchronous speed is not zero but negative. This means that the motor is actively braking at synchronous speed.

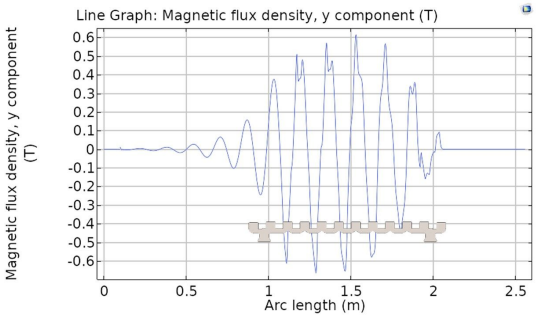

Figure 8: Field profile along the rail. The iron core transversal profile has been overlapped in order to show the magnetic field profile with respect to the LIM.

Since the linear inductors have a finite length, a magnetic fringe field appears at both ends of the motor and it affects the thrust and consequently the final performance. In particular, the magnetic field has to be induced in the rail in front of the motor as the primary advances through a not-yet-magnetized secondary. The reactive power is lost in the rail and tend to decrease the induced currents in it. This effect is present in the front (right side of the plot) and decrease the magnetic flux leading to a decrease of thrust. Moreover, depending on the speed, the induced currents in the rail are still present after that the motor

has passed and they extend up to three times the length of the motor (Figure 8). One of the goals of the study was to evaluate which frequency had to be applied at each speed in order to get the maximal trust. In Figure 9 various curves of thrust for a given speed and in function of the frequency are represented.

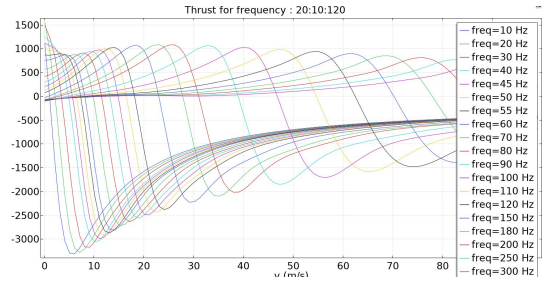

Figure 9: Thrust characteristic for a set of speed with respect to supply frequency.

The peak of each curve gives the right frequency to apply for a given speed. This study has been of paramount importance to build a look-up table of speed vs supply frequency. This allowed the *Voltage Source Inverter (VSI),* supplying the motor, to apply the correct frequency to the motor and thus obtaining the maximum mechanical power during the run.

a. Comparison with measurements

i. Test-bench

A test bench has been designed in order to test the motor at full speed and power. It consists of a large aluminium disc with the same thickness of the SpaceX Hyperloop rail and it allows to mimic the passage of the rail in between the inductors (Figure 10). The radius of the disc has to be large compared to the pole pitch of the motor to limit the curvature effect. In this case, the size of the disc was limited to 2.1 m in diameter because of production limits. However, the radius where the current is induced into the disc was about 0.9 m for a motor length of 0.6 m and a motor height of 68 mm.

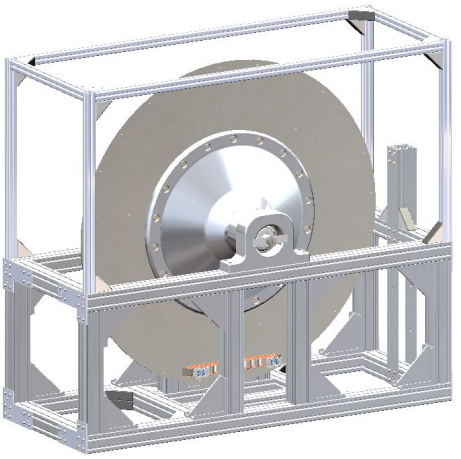

Figure 10: Cad drawing of the test bench.

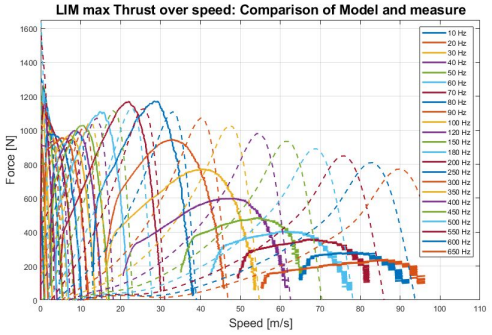

Figure 11: Comparison of the experimental (continuous) and simulated (dashed) thrust characteristic for a set of speed with respect to supply frequency realise on test bench.

Figure 11 shows the comparison between COMSOL simulations and measured data on the test bench. One can see that the thrust characteristics are in good agreement at low frequencies and differ for higher speeds. This can be because the VSI reached its limit in terms of apparent power. As the equivalent impedance of the motor increases with the frequency due to its inductive part, the VSI reaches the maximum output voltage and the requested current can not be supplied. Thus, the current applied above 30 m/s is below the requested one (i.e. 830 A in this case) and the thrust differs from the one simulated. Nevertheless, this result confirm the validity of 2D FEM model, within the expected limitations of conducting the analysis in constant current.

ii. Run on the rail at EPFL and at the SpaceX Hyperloop competition

The day of the competition, our pod has finally been tested on the rail during the extreme conditions for which it has been designed. In fact, alongside the LIM design, our team performed accurate FEM studies in COMSOL on the mechanical, stability and thermal behaviour of the pod, the results of which have been presented at the Cambridge COMSOL Conference 2019. In Figure 12 we present the thrust in function of the speed and for different frequencies, comparing the 2D model and the measurements carried out the day of the competition. For the whole range of frequencies and speed the simulations reflect with a good accuracy the behavior of the motor. The simulations are taking into account several complexities such as non-linear magnetic materials and complex geometry. The discrepancies however are not trivial to explain. The material properties can play a role, as well as the experimental conditions where the measurements have been performed. During the run, mechanical instabilities can significantly affect the efficiency of the motor. For low speed, when the acceleration is the highest, some oscillations of the pod occurring along the rail, can affect the distance between inductor and rail, reducing dramatically the thrust. For higher speeds the stability system damped such oscillations setting to a more fixed value such distance. This is possible to notice looking at the oscillating thrust in Figure 11 for low speed and frequency, while in the test bench in Figure 10 this did not occur. Eventually, the oscillations at low speed can be linked to measurement noise. In fact, due to the way the thrust has been calculated (not directly measured), the noise has been propagated alongside the numerical integration.

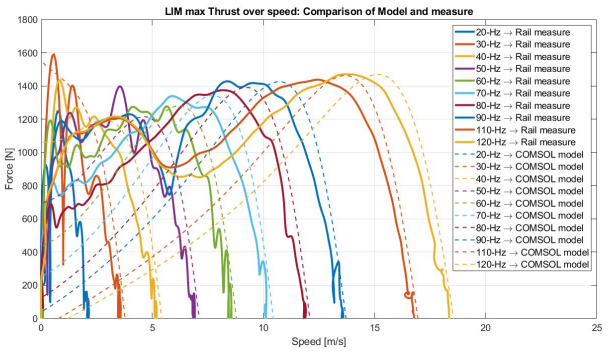

Figure 12: Comparison between experimental measurements and 2D FEM simulation.

5. Conclusion

The use of COMSOL was of paramount importance for the design and optimization of the motor. Parameterizing the design, it has been possible to run quickly and flexibly the simulations until a convergence, dictated by a design goal has been reached. The comparison between measurements and simulations present some discrepancies. The next steps want to include an evaluation of the phenomena inferring these discrepancies. Those can be due to the uncertainty of the material properties or other experimental conditions. Another possibility is the uncertain evaluation of the equivalent impedance of the motor. In fact, by using a Voltage Source Inverter/VSI rated for a given apparent power, this would define how much current can flow in the windings. However, for the level of accuracy and performances obtained, the simulations have been successfully validated showing how the software provided a precise estimation of the motor performances.

6. Acknowledgments

The authors want to thank EPFL, our advisors, professor Marcel Jufer, COMSOL Switzerland and in particular Sven Friedel and Anna Juhasz for the unconditional support, passion and expertise that greatly assisted us during the EPFLoop adventure. COMSOL was one of the main sponsors of this journey since the beginning and helped us to build a reliable prototype with an excellent understanding of its behavior.